Response to Reviewer 1st – Manuscript gmd-2025-268 "Towards an integrated inventory of anthropogenic emissions for China " by Zhang et al., 2025

We would like to thank the reviewer for the careful reading and suggestions to improve the clarity and quality of the manuscript. Below, we provide a detailed reply to each of the comments (Reviewers' comments/questions in bold black, our reply in black, and new text in the manuscript in blue).

Comment 1. Why does the study rely solely on MEIC for China in all harmonized emission inventories instead of using global inventories? The paper devotes substantial effort to harmonizing emission sectors, VOC speciation, and spatial resolution, but these harmonized datasets are not fully utilized to produce the final emissions inventory. Does MEIC significantly outperform the global inventories in China? I did not see supporting evidence for this in Figures 6–7.

We would like to thank the reviewer for their valuable and insightful comments. In our study, we created our final inventory (CINEI) by combining the harmonized national MEIC inventory for mainland China with the global CEDS inventory for regions surrounding mainland China, as described in the manuscript (referred to as HMEI). CINEI also incorporates additional contributions from global inventories, specifically from the agriculture, shipping, and waste sectors. Furthermore, we applied a localized non-methane volatile organic compound (NMVOC) speciation profile within CINEI. For mainland China, we exclusively use MEIC data across all harmonized emission inventories. This choice is based on the fact that MEIC utilizes the most recent and region-specific data for China, including updated emission factors, detailed activity data (such as power plant locations and population), and current mitigation measures (see Section S2). Our study integrates emission estimates derived using these unique factors for all major sectors into the overarching framework of global inventories. As a result, MEIC emissions often differ in magnitude from those reported by other global inventories.

Following the suggestion of the second reviewer, we have updated Table 2 by adding a column labeled 'Selection Principles'. This new column clarifies the criteria we used to select the main sectors (transportation, industry, power, and residential) from the national MEIC inventory.

To address the second part of the comment (model performance), we have now included detailed model validation metrics in Supplementary Section S13, Figures S27–S28. While some deviations between modeled and observed values (see Figures 6–7) can be attributed to spatial averaging, we have now added the Normalized Mean Bias (NMB) directly to these figures for clarity.

- **Winter (Jan 2017):** The MEIC-based HMEI outperforms all other global inventories for multiple pollutants. For ozone, HMEI achieves the lowest NMB (-26%) compared to HTAP (-52%), CEDS (-33%), CAMS (-40%), and CINEI (-44%). It also shows the lowest Mean Normalized Bias (MNB = 15.6%) and the lowest Mean Normalized Absolute Error (MNAE = 43.1%). For CO, HMEI comes closest to zero NMB (-24%) and performs well for NO_2. Overall, the strong performance of HM_CEDS makes it the optimal choice for wintertime air quality modeling.

- **Summer (July 2017):** During July, HMEI continues to outperform other global emission inventories, especially in predicting NO_2 and CO. For NO_2, HMEI provides the most accurate results, with a normalized mean bias (NMB) of 0.5%, which is closest to zero among all inventories compared to CINEI (2%), CAMS (-21%), CEDS (-21%), and HTAP (113%). It also achieves the lowest mean normalized bias (MNB = 41%) and mean normalized absolute error (MNAE = 32.8%). For CO, HMEI again stands out with the best performance (MNB = 57.6%, NMB = -34%, MNAE = 34.4%) despite the fact that all inventories tend to underestimate concentrations. Ozone predictions using HMEI show moderate overestimation (NMB = 20.0%, MNB = 17.3%) compared to other inventories (CINEI: 14%, CAMS: -31%), likely due to reduced NO_2 in polluted regions, which may enhance ozone formation through increased oxidant availability and OH-VOC reactions.

Despite this challenge with summer ozone, HMEI consistently delivers the most reliable results across multiple pollutants in both winter and summer, making it the best choice for year-round atmospheric chemical modeling.

Changes made in the manuscript:

3rd paragraph in section 3.1 (Line 337-345) in main text: The power sector is the main driver of the decrease in NO_x emissions for China, contributing 49% to the downward trend with a linear reduction of -0.33 Tg yr^{-1}. In the CINEI , emissions from the power and industrial sectors (for NO_x) and the residential sector (for CO) started to decline after peaking in 2013 (see Table S16). This timing aligns with the emission reduction measures implemented, starting with the 12th Five-Year Plan in 2011 (see Text S1). The improved reflection of mitigation actions in the MEIC inventory comes from accounting for factors such as technology adoption and abatement efficiency (see Text S2 and Table S1), such as energy transition to cleaner resources (Yan et al., 2023). Over the study period, the sectors responsible for the largest reductions in CO emissions were industry (60% of the reduction), residential (29%), and transportation (16%). The main contributors to the observed linear declines in CO were industry (39% contribution, -3.6 Tg yr^{-1}), residential (22%, -1.8 Tg yr^{-1}), and power generation (13%, 0.14 Tg yr^{-1}).

2nd paragraph in section 3.4 (Line 456-462) in the main text: Further, we investigate ~~that~~ the comparison of experiments' performance between MEIC-based HMEI and global inventories. Modeling ozone mixing ratio using HMEI in January 2017 achieve the smallest normalized mean bias (NMB = -26%), compared with HTAP (-52%), CEDS (-33%), and CAMS (-40%) (Fig. 7). In July 2017, models using HMEI produced NO_2 and CO bias values (NMB = 0.5% for NO_2, -34% for CO) that are closer to zero than results from global inventories (Fig. 6). Comprehensive analysis using several statistical metrics (NMB, MNB, MNAE, MAE, MFE) consistently demonstrates that HMEI delivers superior overall performance compared to individual global emission inventories (Fig. S27-S28). These comparisons of evaluation metrics suggest that CINEI is based on emissions from the main sectors in the MEIC inventory.

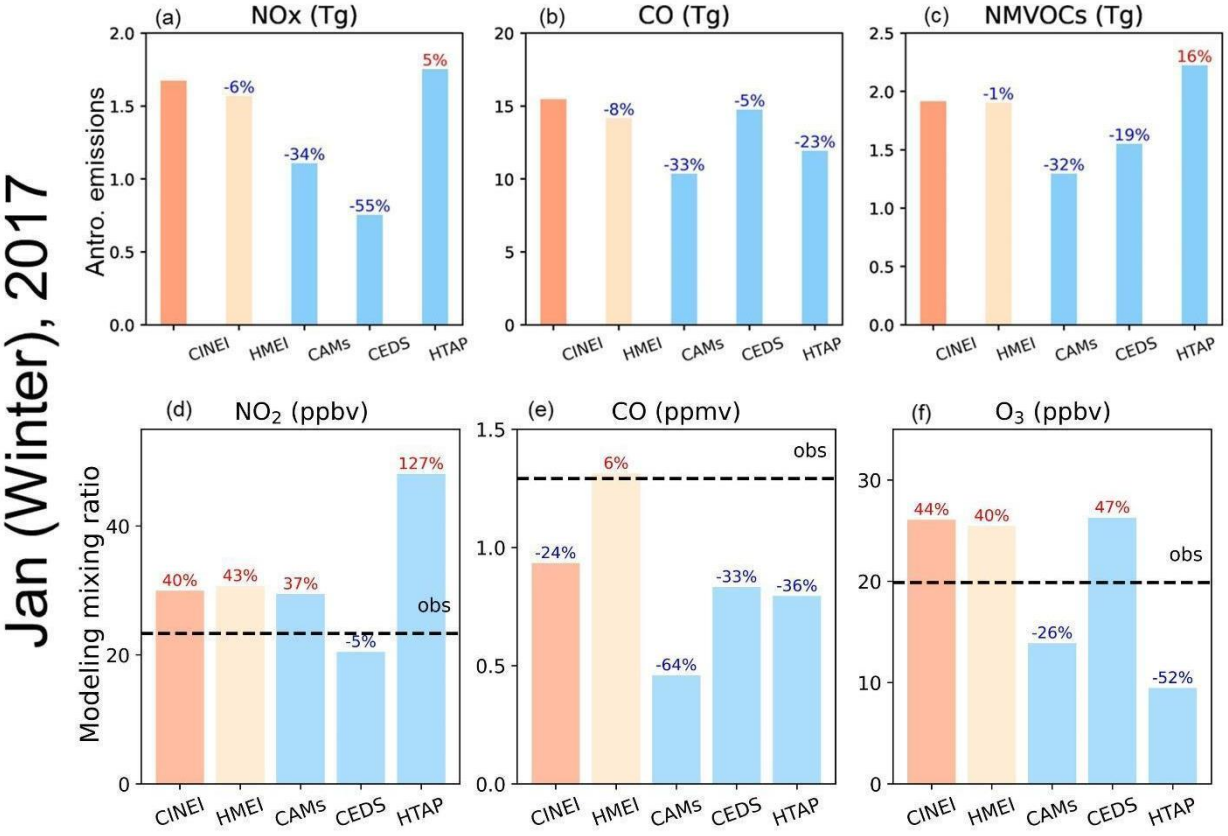

Page 25 in the main text: Figure 6: The top panels (a-c) present total anthropogenic emission differences of ozone precursors (NOx, CO, and NMVOC) for July 2017 between the CINEI, HMEI, CAMS, CEDS, and HTAP inventories using the CINEI integrated emission inventory as a reference. Bottom panels (d-f) show WRF-Chem simulated mixing ratios of O_3, NO_2, and CO for the same month and within the modeling domain (latitudes from 25.5° to 43.6°; longitudes from 103.5° to 127.6°) using the different emission inventories. Individual columns show simulated mean mixing ratios in the model domain for each emission inventory used. The dashed blue lines show average observed mixing ratios calculated using the stations within the specified domain. The numbers shown in the columns represent the normalized mean bias (NMB) against observations

for each modeling experiment, as defined in the first line of Table S7. Values in red indicate overestimation, while values in blue indicate underestimation.

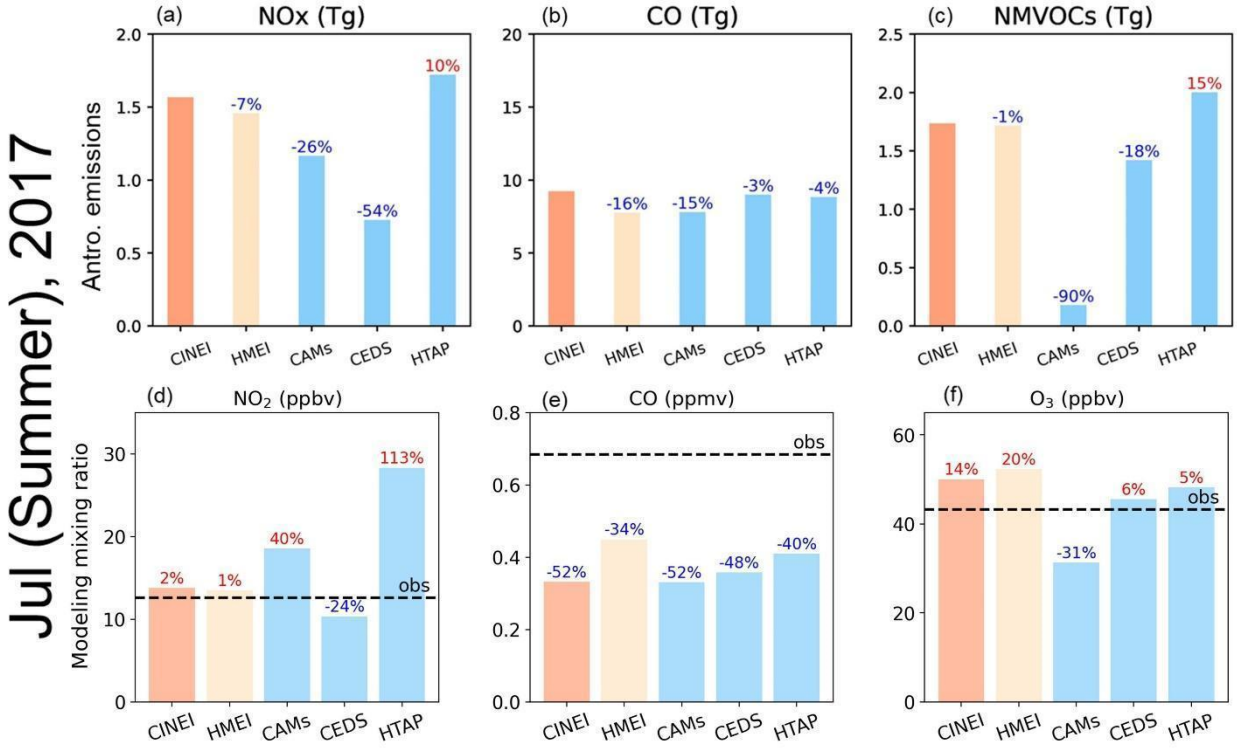

Page 26 in the main text: Figure 7. Same content with Figure 6, but in July 2017.

Comment 2. Additionally, the key distinction between CINEI and MEIC lies in the inclusion of previously missing sources in CINEI, such as agricultural, waste, and marine sectors. While MEIC has been evaluated in previous studies, the current evaluation of CINEI essentially serves to assess the impact of these additional sources. This important insight should be emphasized more clearly and consistently throughout the manuscript.

We thank the reviewer for this suggestion. The key distinction between CINEI and MEIC is indeed the inclusion of agricultural waste and marine (shipping and aviation) sectors, and applying new NMVOC speciated profiles to NMVOC emissions. Our modeling evaluation based on CINEI in this study reveals several differences when compared to previous studies using MEIC and to harmonized MEIC with CEDS inventory (HMEI) in this work. Below, we summarize the improvements associated with these changes in CINEI:

Modeling evaluation:

- In January (Winter), CINEI total emissions over China are (slightly) higher than HMEI: +6% for NO_x, +8% for CO, and +1% for NMVOCs. This increase is due to the inclusion of agricultural, waste, and shipping emissions that are absent in the original MEIC inventory. The additional emissions lead to a small increase in O_3 (less than 1 ppb), along with slight decreases in CO (by 0.4 ppm) and NO_2 (by 1 ppbv) mixing ratios. The improvement for NO_2 is shown by a decrease in normalized mean bias (NMB) from 24% (HMEI) to 22% (CINEI). Other metrics, such as MAE, MNB, and MFE, also support the improvement for NO_2.

- In July (Summer), CINEI shows (slightly) higher emissions compared to HMEI: +7% for NOx, +16% for CO, and +1% for NMVOCs. The added emissions increase O_3 by 3 ppb but lower CO (by 0.17 ppm) and NO_2 (by 2 ppbv). For O_3, the NMB improves from 21% (HMEI) to 12% (CINEI), as supported by additional evaluation metrics.

Impact of additional sectoral emission contributions:

The CINEI inventory includes previously missing sectors for NOx and CO emissions. Based on our results:
- The shipping sector is identified as a key sector for NOx emission in China, because the linear emission change rate of shipping NOx is +0.07 Tg yr^{-1} and it ranks as the 3rd largest contributor to the total trend (21%).
- The aviation sector is also a key sector for NOx emission due to being the 4th contributor to the total trend (3% and +0.01 Tg yr^{-1}).
- Waste CO emission is the 4th largest contributor (13%) to the total trend and has an increasing trend (linear slope: +0.15 Tg yr^{-1}).

4th paragraph in section 3.1 (Line 351-359) in main text (sectoral emission): Ozone precursor emissions from four key sectors not included in the MEIC inventory (shipping, waste, agriculture, and aviation) are included in the CINEI inventory and are identified as key contributors (see Tables S12-15 and Text S8). The shipping sector is a major contributor to NO_x emissions in China, with a linear emission increase of +0.07 Tg yr^{-1} , making it the third-largest driver of the total NO_x trend at 21%. Aviation follows as the fourth-largest contributor to NO_x with 3% (+0.01 Tg yr^{-1}), while waste accounts for the fourth-largest share of the CO trend at 13% and also shows a rising trajectory (+0.15 Tg yr^{-1}, see Table S13). For comparison, NO_x emissions from shipping in the HTAP inventory also display an upward trend of +0.1 Tg yr^{-1} (Table S12), which appears to counteract reductions from the energy sector. In summary, our findings indicate that shipping, waste, aviation, and agriculture are key sectors that influence overall trends, often showing increases where other major sectors have declined.

3rd paragraph in section 3.2 Line 398-404 in main text (NMVOC emission): All of the major NMVOC species identified by CINEI show increasing trends within the sectors added from global inventories, namely agriculture, shipping, aviation, and waste. For example, total NMVOC emissions from the agriculture sector are slightly rising by +0.003 Tg yr^{-1}. Key speciated NMVOC emissions from these four sectors, such as ethene (which contributes 8% to total OFP) and formaldehyde (5%), also show notable increases. To effectively reduce ozone levels, mitigation strategies should target not only highly reactive species like m/p-xylene,

toluene, and propene from industrial sources, but also address emissions from sectors like agriculture and aviation that are often overlooked in national inventories.

The last paragraph in section 3.2 Line 418-426 in the main text (NMVOC speciation): When compared to the national inventory (MEIC, with the same ratio as the harmonized inventories), the ethane-to-acetylene and propene-to-acetylene ratios in CINEI are closer to the observed ratios (Fig. S17). These findings may be linked to two factors. First, the ethane-to-acetylene ratio in CINEI is higher than the MEIC ratio resulting from the incorporation of missing sectors (agriculture, aviation, ships, and waste), which contribute 13% to the total annual average emission and are richer in ethane. Second, the propene-to-acetylene ratio in CINEI is lower than the MEIC ratio despite a 3% additional contribution from these missing sectors. This may be due to the speciated profile used in CINEI (Mo et al., 2018), which attributes a smaller share of emissions to diesel vehicles (mainly emitting alkenes) and a larger share to gasoline vehicles (mainly emitting alkanes) (Table S20). These findings suggest that using local NMVOC speciated profiles can better capture changes caused by current energy transitions and evolving consumption patterns (Yan et al., 2021).

3rd paragraph in section 3.4 (Line 473-477) in main text (Modeling evaluation): The differences between the two emission inventories can be attributed to the inclusion of shipping, waste, and aviation emissions, as well as updated NMVOC speciation in the CINEI dataset. Accounting for these sectors results in a modest increase in total emissions (less than 10%) in CINEI. This change leads to improved model performance, as shown by a reduction in the normalized mean bias (NMB) for ozone in summer (from 21% with HMEI to 12% with CINEI) and for NO_2 in winter (from 24% with HMEI to 22% with CINEI).

Comment 3. Section 3.2 and Figure 4a: What causes the large year-to-year fluctuations in ozone formation potentials (OFPs)?

The ozone formation potential (OFP) measures how much each volatile organic compound (VOC) can contribute to ozone creation. It is expressed in Tg of ozone (Tg-O_3) yr^{-1}. OFP for each VOC species is calculated by multiplying that species' emissions by its maximum incremental reactivity (MIR). Year-to-year changes in OFP depend, therefore, on (1) the reactivity of different NMVOC species, as measured by their MIR (Carter, 2015), and (2) each species' share of total OFP. Trends in emissions of individual NMVOCs are closely linked to their relative abundance and the dominant emitting sectors. Figure 3 displays OFP and emission trends for the major (top 20) VOC species contributing to total OFP from 2008 to 2020.

China's total NMVOC emissions and OFPs, summing all species, increased from 2008 to 2020, with linear trends of 0.2 Tg yr^{-1} for emissions and 1.1 Tg-O_3 yr^{-1} for OFP (Figure S14). Fourteen of the top 20 species (70% contribution of total emission) showed increasing trends and now make up large portions of OFP, including m/p-xylene (18% of OFP, 0.04 Tg yr^{-1}), propene (18%, 0.2 Tg yr^{-1}), and toluene (10%, 0.03 Tg yr^{-1}). The main sources driving this increase are industrial activities such as industrial painting, iron and steel manufacturing, and architectural coatings (Figure S12).

Some sources like aviation, shipping, and waste, though lower in emissions, also contribute to the overall upward trend. Small decreasing trends can be found in species including i-pentane (-0.005 Tg yr^{-1}), formaldehyde (-0.004 Tg yr^{-1}) and trans-2-butene (-0.002 Tg yr^{-1}). The residential and transportation sectors lead the decreasing trends, but fail to offset the emission increase by the other sectors in the study period. Above all, OFPs increase is driven by high-reactive species like m/p-xylene, toluene, and propene from industrial sources, and slightly from the missing sources (aviation and shipping, etc) by national inventory (MEIC).

3rd paragraph in section 3.2 (Line 389-398) in main text: Total NMVOC emissions and OFPs in China, showed an overall increasing trend from 2008 to 2020, with linear slopes of 0.2 Tg yr^{-1} (emission) and 1.1 Tg-O_3 yr^{-1} (OFPs), as shown in Fig. S14. Fourteen of the top 20 species exhibited increasing trends and contributed significantly to OFPs, including m/p-xylene (18% OFP contribution and 0.04 Tg-O_3 yr^{-1}), propene (18% and 0.2 Tg-O_3 yr^{-1}), and toluene (10% and 0.03 Tg-O_3 yr^{-1}) (Fig. S15 and Fig. S16). The primary driver for this increase was the industrial sector, particularly processes like industrial painting, iron and steel production, and architectural coating (Fig. S12). To mitigate ozone formation, targeted strategies should focus on industrial emission controls for high-OFP species, particularly aromatics like xylenes and toluene, while continuing to strengthen transportation and residential emission reductions. Additionally, since formaldehyde and several alkenes showed decreasing trends, policies should maintain these reductions while preventing industrial sector growth from overwhelming the overall mitigation efforts through stricter industrial VOC controls and cleaner production technologies.

The last paragraph in section S10 (Line 276-281) in SI: Based on the VOC emissions analysis from 2008-2020, the overall mean increase in OFP, of 1.3% annually, was primarily driven by significant growth in industrial emissions, which increased by 3.9% yr^{-1} across most VOC species. This industrial growth more than compensated for the decreasing trends in transportation (-3.3% annually) and residential (-2.2% annually) sectors. The species contributing most to ozone formation, m/p-xylene (17.7% of total OFP), propene (16.7%), and toluene (10.0%), all showed increasing industrial emissions despite reductions from other sectors (Figures S15 and S16).

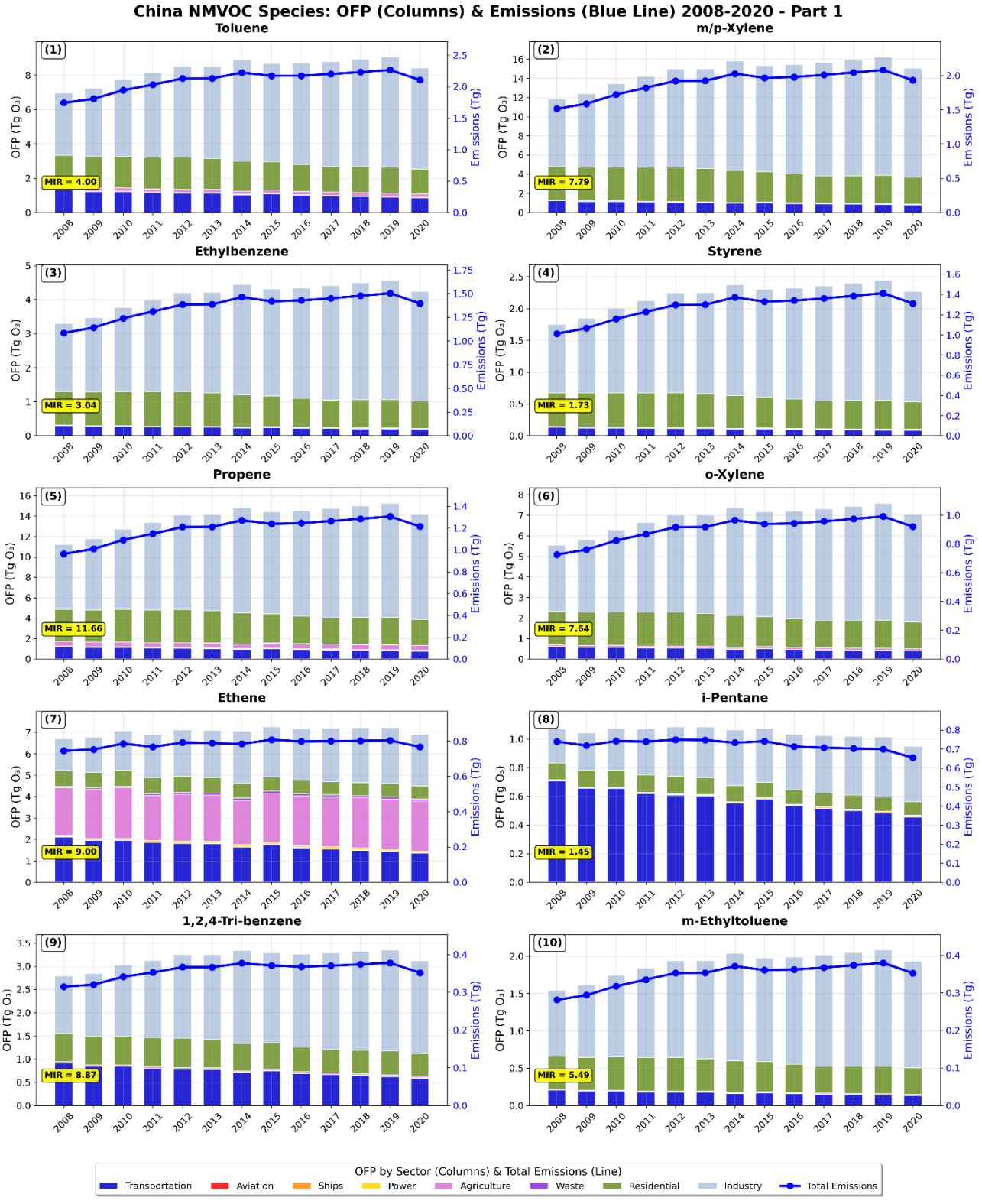

Figure 15. Year-to-year CINEI Ozone formation potentials (OFPs, in columns, unit: Tg-O_3) distinguishing contributions from each sector (see figure legend) and total emission (blue line with dots, unit: Tg) for the TOP-20 important NMVOC species in China from 2008 to 2020. The colors of the columns denote sectors' contribution to OFP.

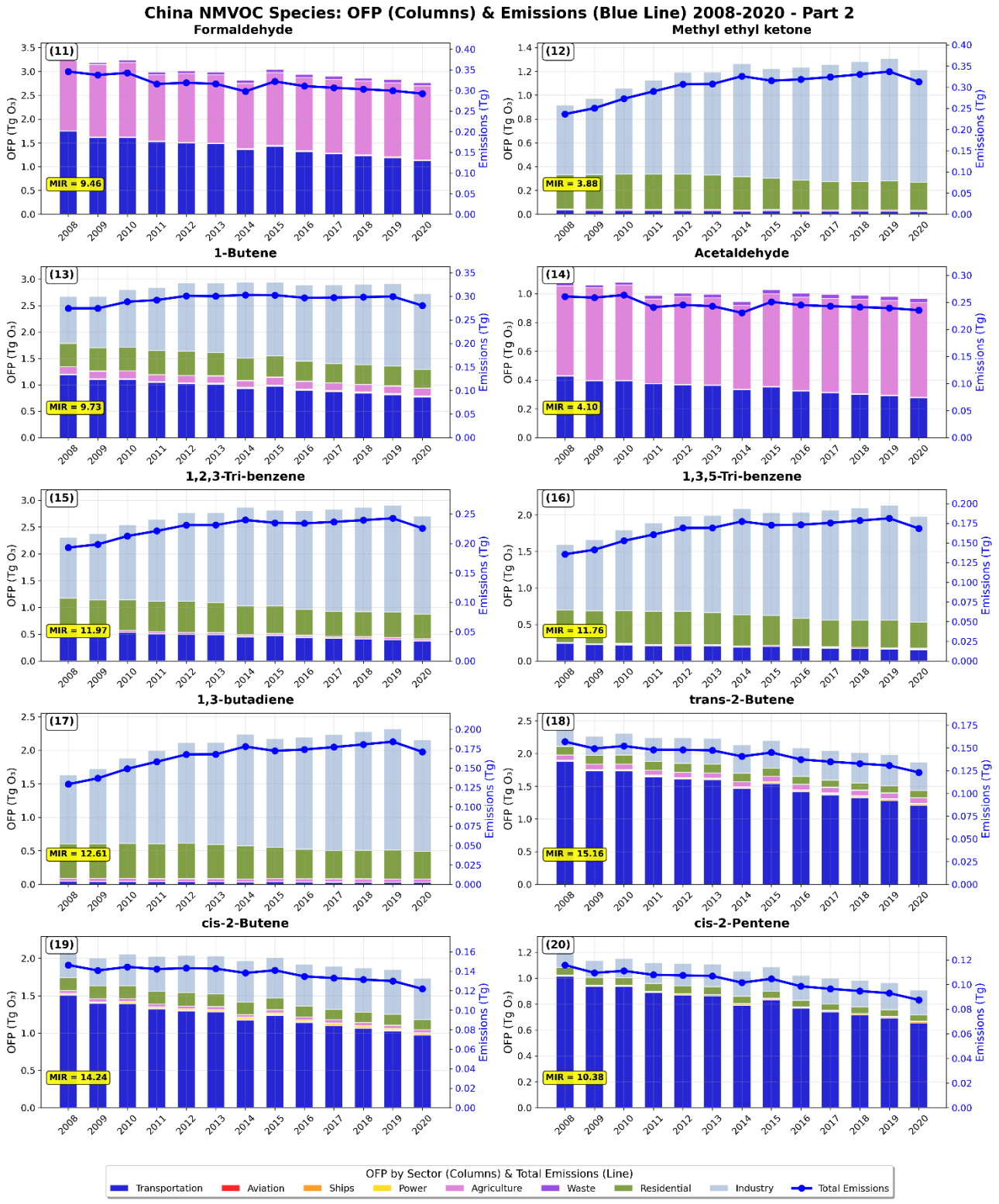

Figure 16. Year-to-year CINEI Ozone formation potentials (OFPs, in columns, unit: Tg-O_3) distinguishing contributions from each sector (see figure legend) and total emissions (blue line with dots, unit: Tg) for the TOP-20 important NMVOC species in China from 2008 to 2020. The colors of the columns denote sectors' contribution to OFP.

Comment 4. How are VOC emissions from volatile chemical products (VCPs) treated in the CINEI inventory?

VCPs represent a specific emission source sector that includes products such as pesticides, coatings, printing inks, adhesives, cleaning agents, and personal care products (McDonald et al., 2018; Seltzer et al., 2021). All of these sources contribute to emissions through evaporation processes. In our approach, we incorporate emissions data for the main sectors from the original MEIC dataset. MEIC classifies VCP emissions into industrial, residential, and agricultural sectors, with examples such as industrial painting, architectural coatings, and printing and dyeing. For transportation, MEIC includes emissions from petrol and diesel vehicles, accounting for both exhaust and evaporation processes.

In CINEI, we categorize VOC emissions from VCPs in two ways: by emission sector and by VOC speciation source profile. First, we obtained total NMVOC emissions from national and global inventories for relevant sectoral emissions. Then, we map emitting sectors to the source profile categorization and use source profile scores to calculate emissions for each species. Finally, we grouped similar species into the MOZART model species.

3rd paragraph Section 2.2 (Line 163-167) in the main text: Emissions from by-product industrial processes include emissions from solvent volatilization, cement, iron and steel production, fugitive emissions, refinery emissions and other fuel-related emissions. This sector also covers emissions from volatile chemical products (VCPs) such as petrochemical products, coatings, and printing inks. These sources emit~~s~~ high-reactivity species such as m/p-xylene, propene, and toluene, which are important contributors to ozone formation.

The last paragraph Section 4 (Line 551) in the main text:
The new version of CINEI will incorporate additional emerging sources, such as new volatile chemical products (VCPs), including the production of personal care products in industry and the use of pesticides in agriculture (Seltzer et al., 2021; Cai et al., 2023).

Reference

Seltzer, K. M., Pennington, E., Rao, V., Murphy, B. N., Strum, M., Isaacs, K. K., and Pye, H. O. T.: Reactive organic carbon emissions from volatile chemical products, Atmospheric Chemistry and Physics, 21, 5079–5100, https://doi.org/10.5194/acp-21-5079-2021, 2021.

McDonald, B. C., de Gouw, J. A., Gilman, J. B., Jathar, S. H., Akherati, A., Cappa, C. D., Jimenez, J. L., Lee-Taylor, J., Hayes, P. L., McKeen, S. A., Cui, Y. Y., Kim, S.-W., Gentner, D. R., Isaacman-VanWertz, G., Goldstein, A. H., Harley, R. A., Frost, G. J., Roberts, J. M., Ryerson, T. B., and Trainer, M.: Volatile chemical products emerging as largest petrochemical source of urban organic emissions, Science, 359, 760–764, https://doi.org/10.1126/science.aaq0524, 2018.

Mo, Z., Shao, M., Liu, Y., Xiang, Y., Wang, M., Lu, S., Ou, J., Zheng, J., Li, M., Zhang, Q., et al.: Species-specified VOC emissions derived from a gridded study in the Pearl River Delta, China, Scientific Reports, 8, 2963, https://doi.org/10.1038/s41598-018-21296-y, 2018.

Yan, L., Zheng, B., Geng, G., Hong, C., Tong, D., and Zhang, Q.: Evaporation process dominates vehicular NMVOC emissions in China with enlarged contribution from 1990 to 2016, Environmental Research Letters, 16, 124 036, https://doi.org/10.1088/1748-9326/ac3872, 2021.

Cai, Z., Xie, Q., Yang, L., Yuan, B., Wu, G., Zhu, Z., Wu, L., Chang, M., & Wang, X. (2023). A novel method for spatial allocation of volatile chemical products emissions: A case study of the Pearl River Delta. Atmospheric Environment, 314, 120119.

Response to Reviewer 2nd – Manuscript gmd-2025-268 "Towards an integrated inventory of anthropogenic emissions for China " by Zhang et al., 2025

We would like to thank the reviewer for the careful reading and suggestions to improve the clarity and quality of the manuscript. Below, we provide a detailed reply to each of the comments (Reviewers' comment/question in bold black, our reply in black, and new text in the manuscript in blue).

Comment 1. Recent efforts, such as HTAP v3.1 (https://essd.copernicus.org/preprints/essd-2024-601/), have also incorporated MEIC for China. It is suggested that the authors compare CINEI with HTAP v3.1 over China to highlight differences and improvements.

Comment 2. Similarly, MIX v2 has integrated MEIC emissions. What are the methodological advancements and advantages of CINEI relative to MIX v2?

We thank the reviewer for the detailed comments on the newly released HTAPv3.1 and MIXv2 emission dataset (Li et al., 2024; Guizzardi et al., 2025) and the suggestion to compare with the here developed inventory in order to further support the usefulness of it.

CINEI introduces methodological improvements and offers a more comprehensive coverage of emission sectors than MIXv2, especially with the inclusion of the agriculture and aviation sectors. In addition, CINEI's detailed NMVOC speciation enhances its suitability for global atmospheric modeling. When comparing the HTAPv3.1, MIXv2, and CINEI inventories, the main advantages of CINEI are:

(1) Broader emission sectors in CINEI, including aviation and domestic ships, are missing from the MIXv2 inventory (see Table 2 in Li et al., 2024). MIXv2 presents only seven broad sectors in gridded format and lacks the detailed 22 subsectors in time series, which are available in MEIC v1.4. As shown in Figures S10–S12, MIXv2 is limited in its ability to analyze subsector emission trends over time and complicates direct sector mapping with global inventories. For example, Table 2 in Li et al. (2024) provides a one-way mapping between MIXv2 and the IPCC code. In contrast, Figure S8 provides a two-way mapping, including one between the CINEI and the IPCC code and one between the existing inventories and the IPCC code. Therefore, the absence of specific sub-sectors complicates direct sector mapping with global inventories. For example, enteric fermentation (3A) is missing in MIXv2, while wastewater treatment and discharge (4D) is omitted in both MIXv2 and HTAP. These missing sub-sectors can be identified and addressed during the screening process.

(2) Updated NMVOC speciation profiles in CINEI that are fully compatible with the MOZART chemistry mechanism, which is widely adopted in air quality studies and regional chemistry and transport models (CTMs), such as the Weather Research and Forecasting (WRF) model coupled with Chemistry (WRF-Chem), the Community Earth System Model (CESM) and the Multi-Scale Infrastructure for Chemistry and Aerosols

(MUSICA) (Dai et al., 2023 and 2024; Mariscal et al., 2025; Tilmes et al., 2019). The MIXv2 inventory provides speciations such as CB05 and SPARC that are suitable for certain regional and chemistry models; while HTAPv3.1 currently lacks local profile updates for NMVOC species and the speciated NMVOC emissions in gridded format have not yet been completed (Guizzardi et al., 2025).

(3) Facilitation of widely used chemistry mechanisms for global climate models. CINEI's integration with the global CEDS inventory further enhances its applicability for climate change studies, including use within the Coupled Model Intercomparison Project (CMIP) framework (Feng et al., 2020). CINEI is compatible with the MOZART chemistry mechanism that is widely adopted in air quality studies and regional chemistry and transport models; This broad compatibility positions CINEI as a flexible and valuable resource for a wide range of modeling applications.

We have added a supplementary Figure S6 that shows a comparison of the interannual variation in NO_x, CO, and NMVOC emissions among CINEI, MIXv2, and HTAPv3.1. For the overlapping period (2010–2017), the inventories show minor discrepancies. On average, annual emissions in HTAPv3.1 are 2.1% higher than CINEI (ranging from -0.8% to +5.8% across different species), while MIXv2 emissions are consistently 3.2% lower (ranging from -1.6% to -6.1%). These differences mainly result from variations in sectoral aggregation methodologies. For instance, NO_x emissions in CINEI and HTAPv3.1 are higher than in MIXv2, with annual differences of 1.5 Tg (5%), mainly due to the omission of aviation (1.1 Tg) and agricultural soil emissions (0.3 Tg) in MIXv2. Annual CO emissions from agricultural waste burning in HTAPv3.1 are 5 Tg higher than in CINEI and MIXv2. Although both CINEI and MIXv2 provide speciated NMVOC emissions compatible with chemistry mechanisms, HTAP currently lacks local profile updates for NMVOC species.

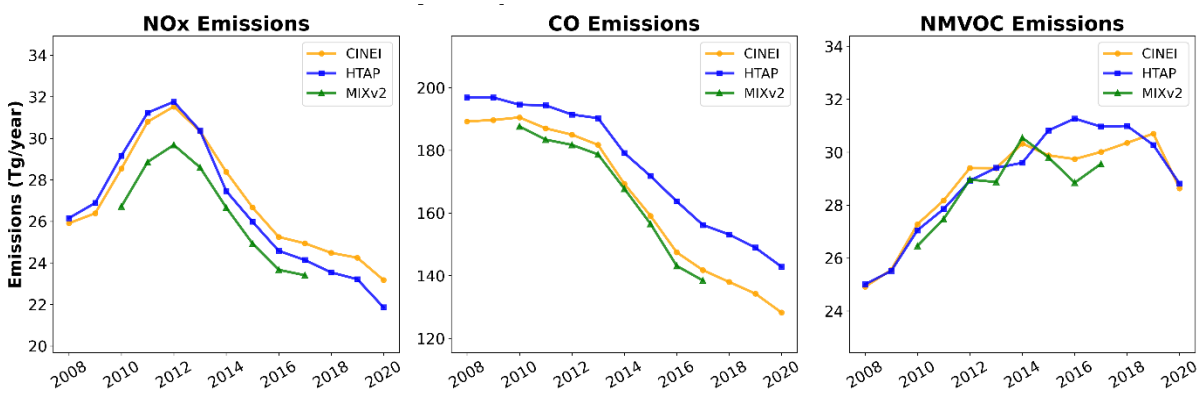

Figure S5. Interannual variability of total NOx (NO_2), CO and NMVOC emissions in China from the CINEI in orange (2008 to 2020) and MIXv2 in green (2010 to 2017), and HTAPv3.1 in blue (2008 to 2020).

We have also performed an additional experiment based on MIXv2 in the summer that showed an underestimation of NO_2 by 7 ppbv (NMB = -54%), CO by 0.5 ppmv (-85%), and O_3 by 14 ppbv (-34%) (Figure S29 and Table S22). The larger discrepancy likely resulted from missing

aviation emissions and reactivity due to lumping together NMVOC species (Li et al., 2024). However, CINEI and HMEI both have consistent speciated NMVOC emission values that align with global inventories, resulting in more reliable model performance. Furthermore, modelling performance based on CINEI in July 2017 outperforms that based on MIXv2, as illustrated in Figure S25 and Table S23. The MIXv2-based runs substantially underestimated all three pollutants: NO_2 by 7 ppbv (-54%), CO by 0.5 ppmv (-85%), and O_3 by 14 ppbv (-34%). These underestimations likely result from (1) missing emission sectors such as aviation and agriculture, leading to lower NOx and CO emissions and (2) incomplete accounting for transported emissions from surrounding regions and the ocean. CINEI integrates China's emissions within the CEDS inventory, while MIXv2 uses other regional inventories (CAPSS for Korea and MOEJ for Japan). Additionally, MIXv2 inventory provides NMVOCs species as high-lumped species, which might lead to missing reactivity of NMVOCs species in WRF-Chem model.

This discussion is added in the supplementary material section S12.

In the revised manuscript we added the following text:

The 4th paragraph in section 1(Line 67) in the main text: Reference to Guizzardi et al., 2025 was added.

The 4th paragraph in section 2.1 (Line 129-138) in the main text:

Our final dataset-CINEI aims at methodological improvements and offers a more comprehensive coverage of emission sectors than MIXv2, especially with the inclusion of the agriculture and aviation sectors. In addition, CINEI's detailed NMVOC speciation that is fully compatible with the MOZART chemistry mechanism enhances its suitability for global atmospheric modeling and its versatility relative to other regional inventories, including MEIC, REAS, and MIXv2. Figure S6, showing a comparison of the interannual variation in NOx, CO, and NMVOC emissions over China among CINEI, MIXv2, and HTAPv3.1 inventories for the overlapping period (2010–2017), demonstrates only minor discrepancies among the inventories. Annual emissions in HTAPv3.1 are 2.1% higher than CINEI (ranging from -0.8% to +5.8% across different species), while MIXv2 emissions are consistently 3.2% lower (ranging from -1.6% to -6.1%) (see further discussion in ~~the~~ section S4 of SI).

Step 3 in section 2.2 (Line 233-234) in the main text: CINEI inventory with MOZART NMVOC speciation can be used in a wide range of air quality studies, as well as in regional and global chemistry and transport models (CTMs). Examples include the Weather Research and Forecasting (WRF) model coupled with Chemistry (WRF-Chem), the Community Earth System Model (CESM) and the Multiscale Infrastructure for Chemistry and Aerosols (MUSICA) (Dai et al., 2023; Mariscal et al., 2025; Danabasoglu et al., 2020). Such compatibility enhances the versatility of CINEI relative to other regional inventories, including MEIC, REAS, and MIXv2.

Supplement

New Figure S6 in Page 9 of SI: Comparison of the interannual variability of total NO_x (NO_2), CO and NMVOC emissions in China between HTAPv3.1, CINEI and MIXv2.

Added discussion text (following) as section S5 (Page 11) of SI:

When comparing the HTAPv3.1, MIXv2 and CINEI inventories, the main advantages of CINEI are:

(1) Broader emission sectors in CINEI, including aviation and domestic ships, are missing from the MIXv2 inventory (see Table 2 in Li et al., 2024). MIXv2 presents only seven broad sectors in gridded format and lacks the detailed 22 subsectors in time series, which are available in MEICv1.4. As shown in Figures S10–S12, MIXv2 is limited in its ability to analyse subsector emission trends over time and complicates direct sector mapping with global inventories. For example, Table 2 in Li et al. (2024) provides a one-way mapping between MIXv2 and the IPCC code. In contrast, Figure S8 provides a two-way mapping, including one between the CINEI and the IPCC code and one between the existing inventories and the IPCC code. Therefore, the absence of specific sub-sectors complicates direct sector mapping with global inventories. For example, enteric fermentation (3A) is missing in MIXv2, while wastewater treatment and discharge (4D) is omitted in both MIXv2 and HTAP. These missing sub-sectors can be identified and addressed during the screening process.

(2) updated NMVOC speciation profiles in CINEI that are fully compatible with the MOZART chemistry mechanism, which is widely adopted in air quality studies and regional chemistry and transport models (CTMs), such as the Weather Research and Forecasting (WRF) model coupled with Chemistry (WRF-Chem), the Community Earth System Model (CESM) and the Multi-Scale Infrastructure for Chemistry and Aerosols (MUSICA) (Dai et al., 2023 and 2024; Mariscal et al., 2025; Tilmes et al., 2019). The MIXv2 inventory provides speciations such as CB05 and SPARC that are suitable for certain regional and chemistry models; while HTAPv3.1 currently lacks local profile updates for NMVOC species and the speciated NMVOC emissions in gridded format have not yet been completed (Guizzardi et al., 2025).

(3) Facilitation of widely used chemistry mechanisms for global climate models. CINEI's integration with the global CEDS inventory further enhances its applicability for climate change studies, including use within the Coupled Model Intercomparison Project (CMIP) framework (Feng et al., 2020). CINEI is compatible with the MOZART chemistry mechanism that is widely adopted in air quality studies and regional chemistry and transport models; This broad compatibility positions CINEI as a flexible and valuable resource for a wide range of modeling applications.

Figure S6 shows a comparison of the interannual variation in NOx, CO, and NMVOC emissions among CINEI, MIXv2, and HTAPv3.1. For the overlapping period (2010–2017), the inventories show minor discrepancies. On average, annual emissions in HTAPv3.1 are 2.1% higher than CINEI (ranging from -0.8% to +5.8% across different species), while MIXv2

emissions are consistently 3.2% lower (ranging from -1.6% to -6.1%). These differences mainly result from variations in sectoral aggregation methodologies. For instance, NOx emissions in CINEI and HTAPv3.1 are higher than in MIXv2, with annual differences of 1.5 Tg (5%), mainly due to the omission of aviation (1.1 Tg) and agricultural soil emissions (0.31 Tg) in MIXv2. Annual CO emissions from agricultural waste burning in HTAPv3.1 are 5 Tg higher than in CINEI and MIXv2. Although both CINEI and MIXv2 provide speciated NMVOC emissions compatible with chemistry mechanisms, HTAP currently lacks local profile updates for NMVOC species.

Furthermore, an additional experiment was performed with the MIXv2 inventory for July 2017. The modeling setup, including input data, was kept consistent for both inventories, except for the anthropogenic emission data, as noted in the main manuscript. Due to limited availability of HPC resources, we were unable to perform simulations for January. A comparison of MIXv2 and CINEI modeling results for July 2017 (Figure S29 and Table S22) shows that CINEI delivers better performance than MIXv2 when compared to observations. In contrast, MIXv2 consistently underestimates concentrations: NO_2 by 7 ppbv (-54%), CO by 0.5 ppmv (-85%), and O_3 by 14 ppbv (-34%). These discrepancies can be attributed to several factors: (1) MIXv2 lacks important sectors, such as aviation and agriculture, which leads to lower NOx and CO emissions; (2) emissions from surrounding regions and the ocean are not fully accounted for, whereas CINEI integrates China's emissions within the broader CEDS inventory, while MIXv2 relies on CAPSS for Korea and MOEJ for Japan. (3) MIXv2 provides NMVOC emissions as broad, lumped categories, potentially missing key reactivity of NMVOCs required for accurate simulation in WRF-Chem.

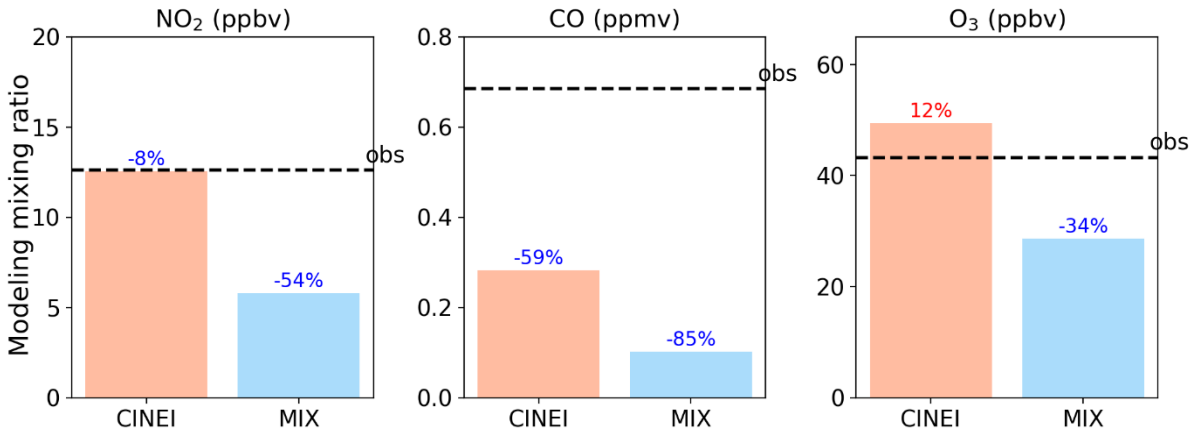

Figure S29. WRF-Chem simulated mixing ratios of O_3, NO_2, and CO for July 2017 (summer) and within the modeling domain using CINEI (in orange) and MIX (in blue). Individual columns show simulated mean mixing ratios in the model domain for each emission inventory used. The dashed blue lines show average observed mixing ratios calculated using the stations within the specified domain. The numbers on the columns are Normalized mean bias (NMB). Blue (red) number indicates underestimated (overestimated).

Table S22. Statistical metrics to evaluate modeling O_3, CO and NO_2 performance based on CINEI and

Metric	O3 (ppbv)		CO (ppmv)		NO2 (ppbv)	
	MIX	CINEI	MIX	CINEI	MIX	CINEI
Observed	43.24	43.24	0.68	0.68	12.61	12.61
Model	28.68	49.46	0.10	0.28	5.79	12.54
NMB (%)	-34	12	-85	-59	-54	-8
MFB (%)	-42	10	-149	-84	-88	-17
MNAE (%)	34	18	85	59	58	34
R	0.95	0.95	0.28	0.50	0.85	0.85

The first paragraph in section 2.3 (Line 278) in the main text: In addition, the MIXv2 inventory incorporates the MEICv1.4 inventory for Asia, which has high lumped speciation and missing aviation emissions. Its modeling performance with the same setup for July 2017 is discussed in the Supplement (figure S29 and Table S22).

The 3rd paragraph in section 3.4 (Line 482-487) in main text: An additional experiment based on MIXv2 in the summer showed an underestimation of NO_2 by 7 ppbv (NMB = -54%), CO by 0.5 ppmv (-85%), and O_3 by 14 ppbv (-34%) (Figure S29 and Table S22). The larger discrepancy of MIXv2 with observations likely resulted from missing aviation emissions and reactivity due to lumping together NMVOC species (Section S12). However, the speciated NMVOC emission values for both CINEI and HMEI are consistent and align with global inventories, resulting in more reliable model performance.

Section S13 (Line 384-390) in SI: Furthermore, modelling performance based on CINEI in July 2017 outperforms that based on MIXv2, as illustrated in Figure S29 and Table S22. The MIXv2-based runs substantially underestimated all three pollutants: NO_2 by 7 ppbv (-54%), CO by 0.5 ppmv (-85%), and O_3 by 14 ppbv (-34%). These underestimations likely result from (1) missing emission sectors such as aviation and agriculture, leading to lower NOx and CO emissions and (2) incomplete accounting for transported emissions from surrounding regions and the ocean. CINEI integrates China's emissions within the CEDS inventory, while MIXv2 uses other regional inventories (CAPSS for Korea and MOEJ for Japan). Additionally, MIXv2 inventory provides NMVOCs species as high-lumped species, which might lead to missing reactivity of NMVOCs species in WRF-Chem model.

Added Table S22 in SI.

Added Figure S29 in SI.

Comment 3. Table 2: When the same emission source exists in multiple global inventories, how is the choice made? For instance, international shipping emissions are available in CEDS, CAMS, and HTAP. Why is CAMS selected in this case? A clearer explanation of the selection principles is needed.

When the same sector appears in different global inventories, we compare the datasets and examine the sources and methodologies behind the emissions calculations. In the CINEI inventory, emissions data for each sector are selected based on two main criteria: (1) the sector must be as complete as possible in terms of included sub-sectors and chemical species (see 'Completion of sub-sectors and species' in Table 2); and (2) the underlying data used for emissions calculations must be high-quality and up to date (see 'Better underlying data' in Table 2). Below is a summary of how leading global inventories meet these criteria:

The HTAP v3 agricultural emissions are more complete than those of the other models and use more up-to-date underlying data. The HTAP agriculture sector includes subsectors such as manure management (NOx), agricultural soils (NOx) and field burning of agricultural residues (CO and some NMVOC species).

Waste emissions from CEDS are more complete than those from other sources. The HTAP waste sector includes the biological treatment of solid waste and the treatment and discharge of wastewater. The main relative species is CO. Emission data from CAMSv5.3 is adopted from EDGAR v5. We prioritize emission data from more complete sectors, and then make further selections based on whether the data is updated.

Shipping emissions are tracked mainly using Automatic Identification System (AIS) data, which combines terrestrial and satellite observations to provide detailed vessel activity. CAMS further refines shipping emissions and routes with the STEAM3 model (Johansson et al., 2017). However, inland shipping data in CAMS is less comprehensive because AIS coverage is limited on inland waterways. HTAP, which builds on EDGAR data, offers an independent sub-sector specifically for domestic (inland) shipping emissions.

Paragraphs 3rd, 4th, and 5th of Section 2.2 in the main text:

Table 2 lists the data sources for CINEI's sectoral emissions and the missing sectors in existing inventories. By following the IPCC sector definitions, we were able to identify sectors that were omitted from certain emission inventories (see Figure S8). We selected the emission sectors from different inventories based on three principles, in the following priority order: (1) whether the sectors included complete sources (sub-sector) and species, as indicated by "Completion of sub-sectors and species" in Table 2; (2) whether the sector used high-quality and updated underlying data for calculating emissions, as indicated by "Better underlying data" in Table 2; and (3) whether the emission estimations for the sectors considered the mitigation measures implemented in China (as discussed in Section S2), which is indicated by "incorporation of pollution mitigation measures" in Table 2.

For CINEI, we retained the emissions from the four existing sectors (transportation, residential, industry, and energy) that were utilized in MEIC, as these sectors adhere to the three principles.

As detailed in Section S2, MEICv1.4 employed local emission factors and activity data and included a parameter for abatement estimation (Section S2 and Table S1). The emission peak year is consistent with the year of mitigation implementation (see Section S7).

We integrated emissions from various global inventories for the four missing sectors to ensure comprehensive sectoral coverage and consistency between national and global emission inventories. Specifically, we used emissions from HTAP for aviation and domestic shipping. We opted for HTAP's data for domestic shipping because its inventory provides an independent sub-sector for inland shipping, whereas inland shipping emissions from CAMS are less complete due to the limited use and coverage of the Automatic Identification System (AIS) on inland waterways. We incorporated ocean shipping emissions from CAMS, which refines data using the Ship Traffic Emission Assessment Model (STEAM3), providing a more detailed representation of shipping routes and emissions (Johansson et al., 2017). For the agriculture and waste sectors, we utilized data from CEDS because its agricultural emissions are more comprehensive than those of MEIC (which only considers NH_3, and its waste emissions are more complete than those from sources from other inventories (Figure S6).

Updated Table 2 as shown below:

Table 2. Data sources of CINEI sectoral emissions and mapping with global emission inventories

Sectors	If provided by existing inventories				CINEI Data Source	Selection Principles***
	MEIC	CEDS*	CAMS	HTAP*		
Power	✓	✓	✓**	✓	MEICv1.4	(1) (2) (3)
Industry	✓	✓	✓**	✓	MEICv1.4	(1) (2) (3)
Residential	✓	✓	✓	✓	MEICv1.4	(1) (2) (3)
Aviation	missing	missing	missing	✓	HTAPv3	(2)
Transportation	✓	✓	✓	✓	MEICv1.4	(1) (2) (3)
International Ships	missing	✓	✓	✓	CAMSv5.3	(2)
Domestic Ships	missing	missing	✓	✓	HTAPv3	(2)
Agriculture	✓**	✓	✓	✓	HTAPv3	(2)
Waste	missing	✓	✓	✓**	CEDSv2021	(2)

* As emissions from HTAP and CEDS are not extended to 2020, we use a linear regression of the emissions from 2008 to 2018 (2019) for HTAP (CEDS) and extrapolate to 2020 for CINEI.

** Indicates that the emissions inventory provides parts of the sectoral emissions but misses some subsectors suggested by the IPCC report. Details on IPCC subsectors and a comparison to each inventory are listed in Figure S6.

*** The selection principles are prioritized in the following order: (1) Completion of sub-sectors and species, (2) Better underlying data, and (3) Incorporation of mitigation.

Added Figure S7 in SI: Spatial distribution of international shipping and inland shipping of CAMs and HTAP.

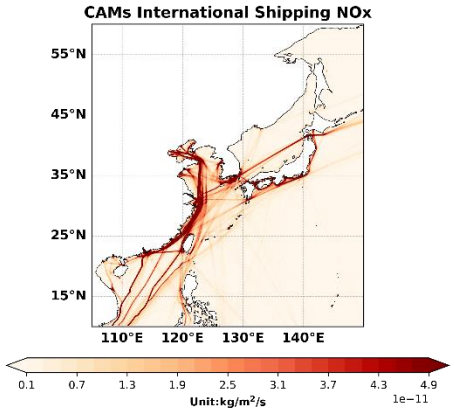

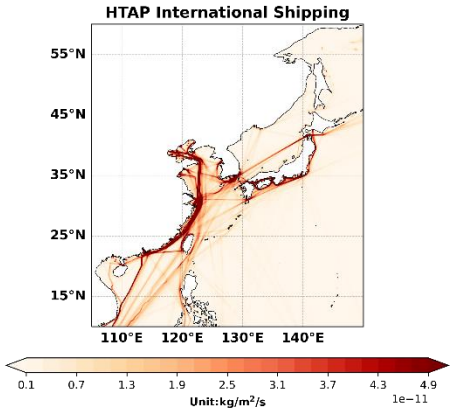

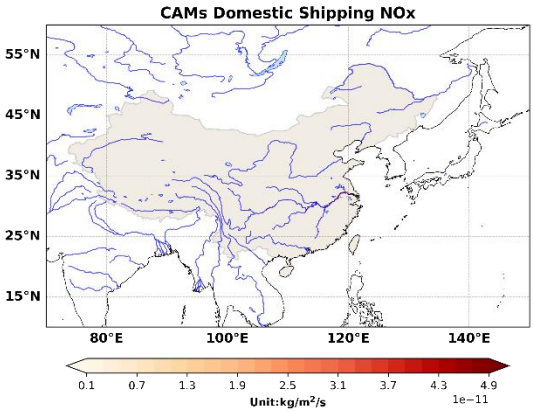

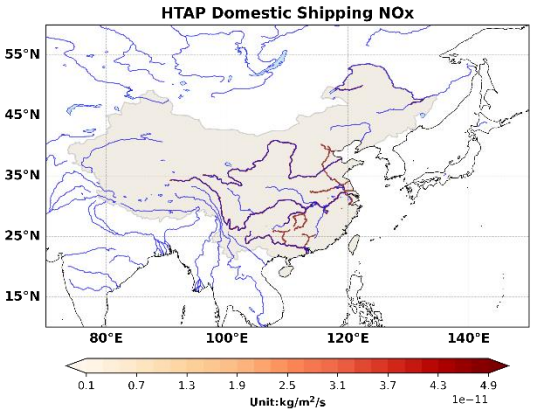

Comment 4. What are the exact differences between HMEI and CINEI? Is it solely the inclusion of previously missing sectors (e.g., ships, aviation, waste, agriculture), or are there additional improvements in sectoral mapping, NMVOC speciation, or spatial harmonization?

We thank the reviewer for highlighting the differences between the HMEI and CINEI inventories. The primary distinction is that the MEIC inventory that the basis of the HMEI inventory for Mainland China does not cover certain sectors—specifically shipping, aviation, waste, and agriculture—while CINEI addresses these gaps by incorporating these additional sources. CINEI also improves NMVOC characterization by utilizing locally observed NMVOC profiles, ensuring that sector-specific compositions are more accurately represented. Furthermore, CINEI uses a uniform sector definition and a consistent spatial resolution of 0.25°, enhancing comparability and spatial detail.

The increase in total emissions in CINEI compared to HMEI is primarily due to the inclusion of these previously omitted sectors (see Figures 3d–f), resulting in average annual increases of 2.7 Tg NOx, 5.2 Tg CO, and 1.4 Tg NMVOCs. CINEI's use of local NMVOC profiles also leads to differences in the chemical composition of emissions, especially for sectors such as agriculture and waste, which contribute notable amounts of propene, ethene, formaldehyde, and acetaldehyde (see Figure 4b).

Section 2.2 (Line 266-268) in the main text: The difference between CINEI and HMEI lies in the new sectors (shipping, aviation, waste, and agriculture) added to CINEI, which increase total emissions. Speciated NMVOCs in CINEI are improved by applying locally observed NMVOC profiles. Furthermore, the additional emission sectors affect the composition of specific local emissions, which will be discussed in later sections.

2nd paragraph in section 3.1 (Line 320-322) in the main text: Compared to MEIC (harmonized inventories) for China, CINEI total emissions on annual average include the contributions of the ships sector to NOx emissions (2.7 Tg), the waste sector to CO emissions (5.2 Tg), and the agricultural sector to NMVOC emissions (1.4 Tg) (Fig. 3d-f).

2nd paragraph in section 3.2 (Line 383-386) in the main text: The agricultural sector is the main source for formaldehyde (52%) and acetaldehyde emissions (60%), related to the emissions along with crop burning (including the burning of rice and wheat straw, maize, etc.). Ignoring agricultural NMVOC emissions in anthropogenic emission inventories can lead to underestimated contributions of these species to ozone pollution. Ozone pollution may occur in areas with intensive local agricultural activity.

Comment 5. The CAMS dataset is extended from 2018 to 2022 using linear slopes from CEDS. How are uncertainties introduced by this extrapolation process quantified and propagated? More detailed treatment or discussion is recommended.

Table 3 summarizes the uncertainties associated with CAMS emissions for the main sectors. Overall, the CAMS extrapolation method introduces between 30% and 60% of uncertainty. The greatest uncertainties are found in the power sector, reaching 96% for CO emissions and 148% for NMVOC emissions. These unusually high values are likely due to systematic uncertainty regarding how CAMS defines the power and industry sectors. In comparison, uncertainties from bottom-up and top-down modeling approaches cited in the literature are lower, typically between 20% and 50%. To reduce uncertainties in future work, we recommend a combined approach that uses activity data, in-situ measurements, satellite observations, and CTM modeling. Section S3 and Table S3 will be added in the supplementary to explain how uncertainties in CAMS emissions due to the extrapolation method are evaluated.

Table S3. Comprehensive uncertainty table for CAMs Emissions Extrapolation Method: CO, NOx, and NMVOC by Sector

Species	Sector	Slopes (Tg/year)			Emission in base year (2018)			σ_model	σ_total
		CEDS	CINEI	σ_slope (%)	CAMs (Tg)	CINEI (Tg)	σ_bias (%)	(%)	(%)
CO	Transportation	-1.6021	-1.5969	0.3	14.83	23.67	45.9	39.0	60.2
	Residential	-2.1838	-2.2927	4.9	27.34	55.81	68.5	39.0	78.8
	Power	0.0692	0.1850	91.1	12.80	5.01	87.5	39.0	95.8
	Industry	-1.3966	-2.2350	46.2	75.49	47.67	45.2	39.0	59.7
NOx (NO2)*	Transportation	-0.0160	-0.1717	165.8	5.2	7.5	35.0	46.0	57.8
	Residential	-0.0229	-0.0267	15.5	1.0	0.8	17.3	46.0	49.2
	Power	-0.1439	-0.2977	69.7	6.3	4.0	44.1	46.0	63.7
	Industry	-0.0956	-0.1608	50.9	8.5	9.1	7.2	46.0	46.6
NMVOC†	Transportation	-0.2747	-0.2145	24.6	3.89	4.63	17.4	26.0	31.3
	Residential	-0.2069	-0.0941	74.9	3.05	4.67	42.1	26.0	49.5
	Power	0.1204	-0.0024	208.2	0.49	0.08	146.0	26.0	148.3
	Industry‡	-0.0046	0.5275	203.5	20.19	19.49	3.5	26.0	26.2

Notes:

* CAMs NOx (represented by NO) emissions scaled by factor 1.5

‡ Industry sector for NMVOC includes solvents (ind + slv)

– Slopes calculated from linear regression (2015-2019)

– Base year emissions in appropriate units for each species

– Uncertainties calculated using equations (2)-(4) from methodology

– Model uncertainties: CO (39%), NOx (46%), NMVOC (26%) from Li et al. (2024).

Add text in section 2.1 (Line 120) in the main text: The uncertainties of CAMs extrapolation method will also be discussed in Section 3.1.

2nd paragraph in section 3.1 (Line 323-325) in the main text: The uncertainties of the CAMs extrapolation method for the main sectors are estimated between 30% and 60% (see Section S5 and Table S3). One exception is the power sector where uncertainty exceeds 100%, likely due to the systematic uncertainty in the sector' definitions and mapping.

Section 4 (Line 540-543) in the main text: In a follow-up study, we will evaluate CINEI's representation of NOx-VOC photochemistry in CTM models and compare the results with observational data. We also plan to incorporate additional observational and modeling approaches to develop an updated version of the CINEI emissions dataset. This will help reduce uncertainties in the emission estimates and minimize modeling biases in CTM applications.

Main text Line 542: We will use more observational data, such as from TROPOMI and in-situ measurements, to constrain the total emissions for ozone precursors and NMVOC speciation.

Add Table S3 in SI:

Add a section S5 in SI:

1. Method to quantify the uncertainties on the projection of CAMs emission from 2018 onward.

For this study, CAMs emissions for the main sectors (industry, power, residential and transportation) from 2018 to 2020 are extrapolated using linear slopes ($slope_{spec,i}$) derived from CEDS for the period 2015 to 2019, with 2018 as the base year. The emissions for a given species (spec) and sector (i) in years 2019–2020 are calculated as:

$$E_{spec,year,i} = E_{spec,2018,i} + slope_{spec,i} \times (year - 2018) \quad (1)$$

Here, $slope_{CEDS,\ spec,i}$ is the slope of linear regression of annual total CEDS emissions for sector i and specific species (spec) from 2015 to 2019 and $slope_{CINEI,\ spec,i}$ is the slope of linear regression of annual total CINEI emissions. The uncertainty of the linear slope is calculated as the absolute difference between linear slopes of CINEI and CEDS from 2015 to 2019 with respect to their averages. The calculation is expressed as:

$$\sigma_{slope} = \frac{|slope_{CEDS,spec,i} - slope_{CINEI,spec,i}| \times 2}{slope_{CEDS,spec,i} + slope_{CINEI,spec,i}} \times 100 \quad (2)$$

The uncertainty of the bias is calculated as the absolute difference of CAMs and CINEI emissions with respect to their average in the base year.

$$\sigma_{bias2018} = \frac{|E_{CAMs,spec,2018,i} - E_{CINEI,spec,2018,i}| \times 2}{E_{CAMs,spec,2018,i} + E_{CINEI,spec,2018,i}} \times 100 \quad (3)$$

The uncertainty of the model (σ_{model}) originates from differences in approaches to calculate emissions, including top-down estimation (satellite estimation and inverse modeling) and bottom-up estimation (Miyazaki et al., 2017; Li et al., 2024; Liu et al., 2016a). This component is independent of the uncertainties of linear slope and base-year emission in bottom-up emission inventories. Adopted from Li et al. (2024), the standard deviation of all estimates on emission trends can be represented by 46% for NOx, 39% for CO, and 26% for NMVOC.

The propagation of uncertainty for three independent uncertainties is expressed as follows:

$$\sigma_{total,spec,i} = \sqrt{\sigma^2_{slope,spec,i} + \sigma^2_{model,spec,i} + \sigma^2_{bias,spec,i}} \quad (4)$$

References

Feng, L., Smith, S. J., Braun, C., Crippa, M., Gidden, M. J., Hoesly, R., Klimont, Z., van Marle, M., van den Berg, M., and van der Werf, G. R.: The generation of gridded emissions data for CMIP6, Geosci. Model Dev., 13, 461–482, https://doi.org/10.5194/gmd-13-461-2020, 2020.

Mariscal, N., Emmons, L. K., Jo, D. S., Xiong, Y., Judd, L. M., Janz, S. J., Chai, J., and Huang, Y.: Evaluation of Ozone and its Precursors using the Multi-Scale Infrastructure for Chemistry and Aerosols Version 0 (MUSICAv0) during the Michigan-Ontario Ozone Source Experiment (MOOSE), EGUsphere [preprint], https://doi.org/10.5194/egusphere-2025-228, 2025.

Li, M., Kurokawa, J., Zhang, Q., Woo, J.-H., Morikawa, T., Chatani, S., Lu, Z., Song, Y., Geng, G., Hu, H., Kim, J., Cooper, O. R., and McDonald, B. C.: MIXv2: a long-term mosaic emission inventory for Asia (2010–2017), Atmos. Chem. Phys., 24, 3925–3952, https://doi.org/10.5194/acp-24-3925-2024, 2024.

Guizzardi, D., Crippa, M., Butler, T., Keating, T., Wu, R., Kamiński, J. W., Kuenen, J., Kurokawa, J., Chatani, S., Morikawa, T., Pouliot, G., Racine, J., Moran, M. D., Klimont, Z., Manseau, P. M., Mashayekhi, R., Henderson, B. H., Smith, S. J., Hoesly, R., Muntean, M., Banja, M., Schaaf, E., Pagani, F., Woo, J.-H., Kim, J., Pisoni, E., Zhang, J., Niemi, D., Sassi, M., Duhamel, A., Ansari, T., Foley, K., Geng, G., Chen, Y., and Zhang, Q.: The HTAP_v3.1 emission mosaic: merging regional and global monthly emissions (2000–2020) to support air quality modelling and policies, Earth Syst. Sci. Data Discuss. [preprint], https://doi.org/10.5194/essd-2024-601, in review, 2025.